Published in final edited form as:
Dev Cell. 2005 July ; 9(1): . doi:10.1016/j.devcel.2005.04.003.

The Dynein Light Chain Tctex-1 Has a Dynein-Independent Role in Actin Remodeling during Neurite Outgrowth

Jen-Zen Chuang[1], **Ting-Yu Yeh**[1], **Flavia Bollati**[3], **Cecilia Conde**[3], **Federico Canavosio**[3], **Alfredo Caceres**[3], and **Ching-Hwa Sung**[2,*]

[1]Department of Ophthalmology, Weill Medical College of Cornell University, 1300 York Avenue, New York, New York 10012

[2]Department of Cell and Development Biology, Weill Medical College of Cornell University, 1300 York Avenue, New York, New York 10012

[3]INIMEC-CONICET, Avenue Friuli 2434, 5016 Cordoba, Argentina

Summary

Coordinated microtubule and microfilament changes are essential for the morphological development of neurons; however, little is know about the underlying molecular machinery linking these two cytoskeletal systems. Similarly, the indispensable role of RhoGTPase family proteins has been demonstrated, but it is unknown how their activities are specifically regulated in different neurites. In this paper, we show that the cytoplasmic dynein light chain Tctex-1 plays a key role in multiple steps of hippocampal neuron development, including initial neurite sprouting, axon specification, and later dendritic elaboration. The neuritogenic effects elicited by Tctex-1 are independent from its cargo adaptor role for dynein motor transport. Finally, our data suggest that the selective high level of Tctex-1 at the growth cone of growing axons drives fast neurite extension by modulating actin dynamics and also Rac1 activity.

Introduction

Typical vertebrate neurons have a single thin axon that can grow very long and multiple, thick, tapering dendrites that are comparatively short. Although the extreme polarization of neurons has long been recognized, how neurons develop this polarity remains largely elusive. Specific internal cues that are crucial for polarity determination have been demonstrated in a model system of cultured embryonic hippocampal neurons. In this system, cellular asymmetry develops in the absence of extracellular spatial cues (Fukata et al., 2002a).

Previous studies have suggested that enhancement of neurite elongation directs axon specification (Esch et al., 1999), and modulation of the dynamics of both actin microfilaments and microtubules is likely to be involved in axonal elongation (Fukata et al., 2002c). Pharmacological evidence suggested that actin in the growth cone of the nascent axon is much more labile than that in the growth cones of minor neurites that later develop into dendrites (Bradke and Dotti, 1999). The involvement of enhanced actin-based motility has been further supported by the finding that the RhoGTPase family proteins, key players

*Correspondence: chsung@mail.med.cornell.edu.

Supplemental Data

Supplemental Data include seven figures, two tables, and Supplemental Experimental Procedures and can be found with this article online at http://www.developmentalcell.com/cgi/content/full/9/1/75/DC1/.

in regulating actin cytoskeleton (Ridley et al., 1992), as well as various effectors and guanine nucleotide exchange factors of RhoGTPase proteins have drastic effects on neurite extension (reviewed in Fukata et al., 2002c). It is generally thought that Rho is a negative regulator and Rac is a positive regulator of neurite growth. Nevertheless, little is known about how the local activation (or inactivation) of these RhoGTPase family proteins is regulated. Very recent data suggest that selective enrichment of mPar3/mPar6/atypic protein kinase C complex and phosphatidylinositol 3-kinase activity at axonal neurites may play a crucial role in axonal specification through a mechanism upstream of RhoGTPase-mediated cytoskeletal modulation (Shi et al., 2003).

Microtubules are also involved in establishing axonal polarity. This idea has been demonstrated by the observation that nascent axons had more stable microtubules (Ferreira et al., 1989) and that more microtubules were selectively shipped into neurites fated to be axons (Baas et al., 1993). More recently, CRMP-2 (Collapsin response mediator protein-2) was found to selectively accumulate in the distal region and the growth cones of nascent axons (Inagaki et al., 2001). CRMP-2's ability to bind free tubulin subunits may assist in microtubule assembly, thereby enhancing axonal neurite extension (Fukata et al., 2002b). The microtubule plus-end binding protein APC (Adenomatous polyposis coli) has also been shown to play roles in nerve growth factor-induced axonal outgrowth through its ability to promote microtubule assembly (Zhou et al., 2004).

Studies on the dynamics of growth cones in *Aplysia* neurons have lent support to the idea that microtubule redistribution into the leading lamellipodium is secondary to F-actin disassembly (Forscher and Smith, 1988). Moreover, evidence suggests that the growing microtubules stimulate actin polymerization via Rac1 activation at the leading edge of migrating fibroblasts (Waterman-Storer et al., 1999). The interaction between the microtubule plus-end binding protein CLIP170 and Rac1 effector IQGAP1 may be involved in these processes of cell protrusion (Fukata et al., 2002a). In contrast to non-neuronal motile cells, the molecular machinery responsible for the coordination between microtubules and microfilaments during neurite outgrowth of the vertebrate neuron is poorly understood.

Cytoplasmic dynein is the major motor protein complex responsible for minus-end, microtubule-based motile processes, and hence for an extremely wide range of cellular events (Hirokawa, 1998). Each dynein complex consists of two heavy chains (DHC) that have ATPase and motor activities, plus a group of accessory polypeptides including dynein intermediate chains (DIC), light intermediate chains, and light chains (Vallee et al., 2004). The intermediate chain links accessory proteins and the dynactin complex (which participates in the processivity and cargo binding of the dynein motor) to the dynein heavy chain (King and Schroer, 2000; Waterman-Storer et al., 1995). Several light chain subunits have been identified (Vallee et al., 2004). Among these light chains, Tctex-1 has clearly been shown to be involved in cargo binding. For example, Tctex-1 binds specifically to the cytoplasmic tail of rhodopsin and links rhodopsin-bearing vesicles to the dynein motor complex for transport (Tai et al., 1999; Tai et al., 2001). However, biochemical evidence revealed that a significant amount of Tctex-1 also exists outside the dynein complex (Li et al., 2004; Tai et al., 1998). To date, the cellular function of the complex-free Tctex-1 and the regulation of Tctex-1 assembly into dynein complex are unknown.

The abundance and expression pattern of Tctex-1 in postmitotic young hippocampal neurons (Chuang et al., 2001) prompted us to examine the role of Tctex-1 in neuronal development. In this report, we investigated the expression and function of Tctex-1 in hippocampal neuronal cultures, and we show that the asymmetric and dynamic distributions of Tctex-1 play an essential role in multiple steps of neuronal morphogenesis. Neurons failed to develop neurites when Tctex-1 was suppressed; Tctex-1 overexpression prevented axonal

polarity formation and induced multiple, abnormally long axon-like neurites. Our data argue that dynein motor activity is not critical for Tctex-1-mediated neurite outgrowth. Finally, our findings support the idea that Tctex-1-mediated neurite development depends on its ability to modulate actin dynamics and Rac1 activity, indicating that Tctex-1 may act as a regulatory link between the microtubule and microfilament cytoskeletons in the growth cones of growing axons.

Results

Tctex-1 Is Enriched in Growing Axons of Cultured Hippocampal Neurons

Within the first 24 hr after plating, cultured hippocampal neurons develop several relatively symmetric minor processes 20–30 μm_{ave} in length (stage 2 cells); Tctex-1 was evenly distributed throughout the cell body and minor neurites during this stage (data not shown). However, during development through stages 2–3, Tctex-1 immunoreactivity increased considerably in the longest neurites that had large growth cones and abundant microtubules (Figures 1A-1C), morphological characteristics of nascent axons. Quantification of Tctex-1 labeling intensity relative to that of tubulin confirmed the Tctex-1 signal had a gradient in nascent axons: low at the proximal end and high at the distal region (Figure 1H). By contrast, very little Tctex-1 signal was detected in the growth cones of minor neurites. At the axonal growth cone, Tctex-1 colocalized with tyrosinated (tyr)-tubulin in the central region (Figures 1A and 1B). However, Tctex-1-labeled puncta were also arrayed on F-actin microfilaments that extended into the peripheral lamellipodial veil (Figures 1D and 1E).

Upon reaching stage 3, Tctex-1's distribution appeared to be even more polarized, as it became considerably enriched in the distal axonal shaft and its growth cone (Figures 1F and 1G). In contrast to Tctex-1, immunolabeling for DHC (see Supplemental Figure S1 available with this article online), DIC, or dynactin subunit $p150^{glued}$ (data not shown) did not reveal any particular enrichment within axons or growth cones. Furthermore, little or no labeling for dynein light chain rp3, a Tctex-1 homolog, was found in young neuronal cultures (data not shown).

Tctex-1 Mediates Neuritogenesis

Antisense (AS) oligonucleotide against Tctex-1 was used to carry out loss-of-function experiments to study its role during hippocampal neuronal development. The reduction of Tctex-1 protein, but not control proteins (e.g., DHC, tubulin), was confirmed by immunoblotting (Figure 2E) and quantitative immunofluorescence (Supplemental Table S1). Almost all cells treated with no oligonucleotide (data not shown) or with a scrambled control oligonucleotide (Figures 2A and 2D) were able to reach stage 2 or stage 3 of neuritic development after 24–36 hr; in contrast, the majority of Tctex-1-AS-treated cells failed to develop neurites (Figures 2B-2D, Supplemental Table S2). The Tctex-1-suppressed neurons had segmented lamellipodia but neither typical neurites nor growth cones. Some Tctex-1-suppressed neurons displayed short, thin $tubulin^{+}$ processes that penetrated the lamellipodial veil (Figures 2B and 2C). Morphometric analysis revealed that although more than 80% of 36 hr control neurons reached stage 3, less than 2% of AS-treated cells reached this stage (Figure 2D, Supplemental Table S2).

Similar results were also obtained by examining neurons with Tctex-1 suppressed by RNA interference. Neurons transfected with Tctex-1-siRNA oligonucleotides, identified by lower levels of Tctex-1 immunolabeling, were almost always associated with cells arrested at stage 1 of neuritic development (Supplemental Figures S2A and S2B).

In order to unambiguously identify neurons targeted with Tctex-1-siRNA, we generated a plasmid harboring both the Tctex-1 hairpin siRNA and the GFP cDNA (i.e., Tctex-1-siRNA/

GFP). The silencing effect of this plasmid was confirmed in both transfected HEK cells (Supplemental Figure S2C) and transfected neurons (Figure 2F). When neurons were transfected with Tctex-1-siRNA/GFP plasmid 2 hr after plating and examined 20–22 hr later, almost all GFP^+ neurons had specific reduction of Tctex-1 immunofluorescence but not tubulin immunofluorescence (Figures 2G-2J, arrows; Supplemental Table S1). Again, the majority of the GFP^+, siRNA-targeted cells failed to develop neurites and arrested at stage 1. These siRNA-targeted cells are neurons because they were labeled by TuJ1 antibody, which recognizes the neuron-specific β-III tubulin. By contrast, control neurons transfected with scrambled control-siRNA/GFP plasmid developed neurites normally (Supplemental Table S2). These results consistently suggested that proper Tctex-1 dosage is essential for the initial events of neurite development, such as neurite sprouting from the spherical cell bodies.

To examine Tctex-1's role in neurite extension, neurons were treated with either Tctex-1-AS or Tctex-1-siRNA/GFP ~15 hr after plating and analyzed 20 hr later. While most of control cells reached stage 3, the majority of Tctex-1-suppressed cells were arrested at stage 2 (Figures 2K-2N; Supplemental Table S2). These results clearly suggested that Tctex-1 suppression could effectively inhibit neurite extension and, hence, suppress differentiation during stage 2–3 development.

Ectopic Tctex-1 Expression Promotes Neurite Outgrowth and Abolishes Neuronal Polarity

Gain-of-function studies were subsequently performed to examine the phenotypes of neurons overexpressing Tctex-1. For controls, dissociated neurons were singly transfected with GFP, GFP-DIC, or Flag-DIC (data not shown) or cotransfected with Flag-DIC and GFP (Figures 3L-3O; Supplemental Table S3). The kinetics of neurite development and the morphological parameters of all control neurons were undistinguishable from those of nontransfected neurons. The cells exhibited normal development through stage 2 (Figures 3D-3I) and stage 3, at which time they developed a single $Tau1^+$ axon and several much shorter minor neurites (Figure 3L).

By contrast, almost all Flag-Tctex-1-transfected neurons displayed multiple abnormally long $Tau1^+$ axon-like neurites (Figures 3A-3C). These $Tau1^+$ neurites were also positive for several other axonal markers including APC, Cdc42, synapsin 1, and synaptotagmin (Supplemental Figures S3 and S4; Zhou et al., 2004; Fletcher et al., 1991; Schwamborn and Puschel, 2004). Statistical analysis confirmed that the axon numbers (Figure 3L) and the lengths (Figure 3N) were significantly higher in Flag-Tctex-1-transfected cells than in Flag-DIC-transfected control cells (also see Supplemental Table S3). Despite the increased numbers of axons, the total number of primary neurites extended from Tctex-1-transfected cells was not significantly different from that of control cells (Figure 3M; Supplemental Table S3). Taken together, these results suggest that the ability of Tctex-1 to enhance neurite outgrowth is rather specific, and ectopic expressin of other dynein subunit such as DIC cannot imitate the axogenic effects mediated by Tctex-1. Furthermore, Tctex-1 over-expression enhanced neurite extension, rather than increased neurite sprouting.

Live neurons transfected with GFP (data not shown) or GFP together with Flag-Tctex-1 (Figures 3J and 3K) were also observed by time-lapse video microscopy and sequential photography. In these experiments, neurite development could be traced in the same cells over a period of time, and our results confirmed the accelerated rate of neurite outgrowth in Tctex-1-expressing neurons.

We then sought to determine whether Tctex-1's ability to promote neurite outgrowth remains throughout neuronal differentiation. For this purpose, neurons at 3 days in vitro (DIV) were transfected with Tctex-1 or GFP and harvested 18 hr later. Flag-Tctex-1-

expressing neurons displayed significantly longer axons ($Tau1^+/MAP2^-$ neurites) than those of GFP-transfected cells (Figures 4A and 4B). The mean length of axons (2113 ± 219 μm) of Tctex-1-transfected neurons was almost 3-fold longer than in GFP-transfected cells (720 ± 38 μm; Table 1). In addition, the 4 DIV Tctex-1-transfected neurons bore more than 2.5_{ave} axons compared to the control neurons with 1.2_{ave} axons (Table 1).

Tctex-1-transfected neurons also had significantly longer and more elaborated $MAP2^+$ dendrites relative to the control neurons (Figures 4C-4L). Quantitative morphometric analysis showed that Tctex-1- and GFP-transfected neurons had 18.6 ± 2.2 versus 8.4 ± 1.8 branches per dendrite, respectively.

Both the axogenic and dendritogenic effect elicited by Tctex-1 appeared to be dosage dependent: neurons transfected with a smaller amount of Tctex-1-expressing plasmid exhibited a less prominent, albeit still statistically significant, effect (Table 1).

Tctex-1-Mediated Neurite Growth Is Dynein Independent

To explore the mechanism underlying Tctex-1-mediated neuritic development, we first asked whether the inhibitory effect caused by Tctex-1 knockdown was related to impaired cargo binding for dynein transport. Our first approach to test this possibility was asking whether interference with general dynein activity by overexpression of dynactin subunit p50 dynamitin (Echeverri et al., 1996) would produce a similar phenotype to that caused by loss of Tctex-1. Consistent with the notion that the centrosomal Golgi localization required dynein motor activity (Corthesy-Theulaz et al., 1992), neurons overexpressing myc-p50 had a dispersed Golgi apparatus (Supplemental Figure S5). Despite that, and unlike Tctex-1-suppressed neurons, neurons transfected with p50 were capable of extending minor neurites and developing an axon (Supplemental Figure S6), even though alterations in neuritic caliber including swellings and a slight reduction of axonal length were commonly detected (data not shown).

To directly test the role of dynein motor activity in neuron development, we performed morphometric analyses on neurons cotransfected with DHC-siRNA and GFP plasmid. The gene silencing and function blocking effects of this DHC-siRNA plasmid has been demonstrated by Shu et al. (2004) and confirmed by us (Supplemental Figure S7). As shown in Figures 5A-5F, 1 DIV neurons targeted with DHC-siRNA developed rather normally through stages 2 and 3, by which time a single axon was extended. Taken together, these results suggested that dynein motor activity was not critically required for the initial elaboration of neurites and/or axon specification. These results further indicated that neither the inhibitory effect of Tctex-1 silencing nor the axogenic effect of Tctex-1 overexpression is likely to be due to its dynein-related role.

Previous biochemical evidence revealed that a pool of Tctex-1 exists that is not associated with dynein complex (Tai et al., 1998). To date, the cellular function of the complex-free Tctex-1 and the regulation of Tctex-1 assembly into dynein complex are unknown. To gain insight into whether the “complex” or the “free” form of Tctex-1 is involved in neurite development, we attempted to identify a Tctex-1 mutant unable to incorporate into the dynein complex and examine its effect on neurite outgrowth and axonal polarity in transfected neurons.

Tctex-1 is assembled into dynein complex through its interaction with DIC (Mok et al., 2001; Tai et al., 2001). The DIC binding region of Tctex-1 has been mapped to the region between amino acids 55 and 95 (Mok et al., 2001). In this region, we detected a consensus protein kinase C (PKC) phosphorylation site at threonine 94 (T94). Because purified Tctex-1 can be phosphorylated by PKC in an in vitro assay (our unpublished results), we reasoned

that it was probable that the phosphorylation at T94 serves as a mechanism regulating its interaction with DIC. Site-directed Tctex-1 mutants having the T94 replaced with alanine (T94A) or glutamic acid (T94E) were generated to mimic the unphosphorylated and the phosphorylated Tctex-1, respectively, and these mutants were then tested for their ability to bind endogenous DIC and dynein complex in transiently transfected 293T cells. Both Flag-wild-type (Flag-WT) Tctex-1 and Flag-T94A, but not Flag-T94E, were coimmunoprecipitated with endogenous DIC using anti-DIC antibody (Figure 5G). Converse experiments consistently showed that anti-Flag Ab coprecipitated DIC from cells coexpressing either Flag-WT or Flag-T94A, but not Flag-T94E (data not shown). The inability of T94E binding to DIC in these experiments predicted that T94E was not able to be incorporated into dynein complex.

The organization of the ectopically expressed Tctex-1 related to the dynein complex was also examined by velocity density gradient sedimentation. Gradient fractions of cell lysates containing transfected Flag-tagged, wt, T94E, or T94A were immunoblotted for p150 ^{Glued}, DIC, and Flag. As shown in Figure 5I, in all cases, both markers for dynein complexes (e.g., DIC) and dynactin complexes (e.g., p150 ^{Glued}) were sedimented at 19–20 S, suggesting that overexpression of Tctex-1 and its mutants did not perturb the integrity of dynein complexes. Moreover, both Flag-WT and T94A cosedimented with the dynein/dynactin complexes at 19–20 S (Figure 5I); immunoprecipitation of these dynein-containing fractions with anti-DIC antibody coprecipitated both endogenous as well as the transfected Flag-WT or Flag-T94A (Figure 5H). These results suggested that the ectopically expressed Flag-WT partially replaced the endogenous Tctex-1 and incorporated into the dynein complex, even though, as predicted, a fraction of Flag-WT and Flag-T94A were detected outside the dynein complexes and distributed on the top of the gradient (fractions 9–12; Figure 5I).

In contrast, Flag-T94E was absent from the dynein-containing 19–20 S fractions but exclusively detected in the light fractions of the gradient. Consistently, only endogenous Tctex-1, but not Flag-T94E, was detected in the DIC immunoprecipitates of the 19–20 S, dynein complex (Figure 5H). These results collectively demonstrated that phosphorylation at T94 may be a mechanism to dissociate Tctex-1 from dynein complexes, and therefore the T94E mutant was only found in the fractions outside the dynein complex pool.

We then examined how overexpression of the T94E and T94A mutant affects neurite extension. Like wt Tctex-1-transfected neurons, 4 DIV neurons ectopically expressing T94E for 18 hr displayed multiple axon-like processes (Figure 5J). Other morphological features induced by T94E were also indistinguishable from neurons transfected with wt Tctex-1. Namely, the axons and dendrites were significantly longer, and the dendrites had more branches compared to those of GFP-transfected control neurons (Table 1). In striking contrast, T94A mutant overexpression did not induce the axogenic/dendritogenic phenotype caused by wt and T94E mutant overexpression (Figure 5K). Altogether, these results argued that the T94 phospho-mimic, complex-free form of Tctex-1 was likely to be an active form of Tctex-1 for the enhanced neurite outgrowth activity. These results provided additional support that the neuronal phenotype caused by Tctex-1 occurs through a dynein-independent pathway.

Tctex-1 Modulates the Actin Cytoskeleton through a RhoGTPase-Dependent Pathway

During the course of the above-described experiments, it became obvious to us that Tctex-1-transfected neurons had consistently less F-actin labeling than control nontransfected neurons, or those transfected with control proteins such as GFP-DIC (Figure 3C versus Figure 3F) or Flag-DIC (Figure 6B). The loss of the F-actin signal was particularly prominent in neurite tips. Quantification of phalloidin-labeled F-actin confirmed these observations (Figure 6A). In fact, the phalloidin staining of Tctex-1-transfected cells closely

resembles that of cytochalasin D-treated neurons, which had no F-actin enrichment at the axonal tip. Moreover, while the tubulin level was normally tapered off at the very distal end of control cells, the tubulin levels were relative constant throughout the distal ends of axons in both Tctex-1-transfected and cytochalasin D-treated cells. Intriguingly, a previous report showed that various treatments that disassemble actin also induce multiple axon-like processes on cultured hippocampal neurons (Bradke and Dotti, 1999). The common phenotypes shared by Tctex-1-transfected and cytochalasin D-treated neurons prompted us to speculate that Tctex-1 may regulate axonal outgrowth by attenuating the stability of actin microfilaments.

It is now well established that RhoGTPase family proteins play pivotal roles in regulating actin cytoskeleton organization (Ridley et al., 1992). Rho and Rac have opposing effects on actin organization and differentially affect neurite outgrowth and axon formation. For example, neurite outgrowth is promoted by Rac1 and inhibited by RhoA (see Luo, 2000; Nikolic, 2002). To test whether Tctex-1-induced neurite outgrowth and axonal formation involve a modulation of actin assembly through a RhoGTPase-dependent pathway, we asked if the constitutively active (CA) form of RhoA (G14V) or the dominant-negative (DN) form of Rac1 (T17N) could reverse Tctex-1-mediated phenotypes in cultured neurons.

As expected (Fukata et al., 2002c), neurons singly transfected with either HA-tagged CA-RhoA (Figures 6D and 6E) or DN-Rac1 (Figures 6F and 6G) mutants displayed a dramatic inhibition of axon extension and formation of $MAP2^+$ dendrites (also see Table 1). However, neurons coexpressing CA-RhoA together with Tctex-1 had a single axon with an average length intermediate between those of neurons singly transfected with CA-RhoA or Tctex-1 (Figures 6H and 6I; Table 1). Similarly, Tctex-1 overexpression partially reversed the inhibition of axon elongation induced by coexpression of DN-Rac1, even though these neurons still failed to elaborate $MAP2^+$ dendrite processes (Figures 6J and 6K). Collectively, these results suggested that Tctex-1-induced phenotypes in neurons mimic Rac1 activation or RhoA inactivation or both.

Tctex-1 overexpression in fibroblasts yielded morphological changes—enhanced membrane ruffle and loss of stress fibers (data not shown)—reminiscent of those induced by the active form of Rac1. Pull-down assay revealed that Tctex-1 overexpression in 3T3 cells induced a ~2-fold increase in Rac1 activity, but not RhoA activity (data not shown), without affecting total Rac1 levels (Figure 6C). Furthermore, converse experiments showed that neurons transfected with Tctex-1-siRNA/GFP had significantly lower Rac1 activity compared to the control-siRNA/GFP-transfected cells (Figure 6C). These biochemical results consistently suggested that Tctex-1 upregulated Rac1 activity.

To further test the possibility that Tctex-1 could regulate the actin cytoskeleton through Rac1 activation, we asked whether CA-Rac1 overexpression could compensate for the Tctex-1-siRNA-mediated inhibitory effect on neurite development. To this end, we first showed that neurons transfected with myc-CA-Rac1 alone induced dosage-dependent phenotypic changes. Cells transfected with a lower amount (1 μg) of CA-Rac1 extended a single long axon and several short minor processes, with growth cones that display prominent lamellipodial veils (Figure 6L). Higher doses of CA-Rac1, mimicking Tctex-1 overexpression, also induced multiple axon-like neurites (2 μg in Figure 6M, 4 μg in Figure 6N). Many of these axon-like neurites exhibited excess lamellipodial “waves,” similar to those described in neurons overexpressing Rac-GEF (guanine nucleotide exchange factor)-Tiam1 (T cell lymphoma invasion and metastasis protein) (Kunda et al., 2001). These structures were not detected in Tctex-1-overex-pressing neurons.

As shown in Figures 6O-6Q, neurons cotransfected with equal amounts of Tctex-1-siRNA/GFP and myc-Rac1-CA plasmids (2 μg each) displayed a single axon with several minor neurites. These results suggested that Rac1 is able to overcome the neuritic inhibitory effected exerted by Tctex-1-siRNA. The minor neurites in these double-transfected cells displayed "veiled" growth cones, closely resembling neurons with lower-level Rac1 overexpression (Figure 6L). These results, together with the preceding results, collectively suggested that the neurite and axon development induced by Tctex-1 was likely to be mediated through Rac1-mediated pathway(s).

Discussion

This report reveals that Tctex-1, a cytoplasmic dynein light chain subunit, plays pivotal roles in multiple steps of hippocampal neuronal development, including neurite initiation, neurite growth, axonal polarity establishment, and dendritic elaboration. We therefore predict that similar or overlapping mechanisms based on Tctex-1 are involved in these cellular events during neuronal morphogenesis. Tight control of the asymmetric and dynamic localization of Tctex-1 during neuronal development appears to be a key element providing forces that shape the neuron. For example, high-level Tctex-1 accumulation in the distal region and growth cones of a given neuron at stage 2–3 empowers that neurite to elicit the fastest growth rate and hence become "committed" to the axonal fate. Conversely, the near absence of Tctex-1 in minor neurites could prevent their growth. However, what happens to the axon, happens later in the minor neurites. Tctex-1 reappears in the minor neurites at stage 4, thereby allowing dendritic extension and branching. The ability of Tctex-1 to affect dendrite development was consistent with Tctex-1 immunoreactivity being readily detected in dendritic shafts in 3 DIV cultures (data not shown), even though Tctex-1 is low in minor neurites of young cultured neurons. The importance of Tctex-1 in neurite development is well correlated with its abundance in fetal brains (Kai et al., 1997) and postmitotic young neurons in adult brain (Chuang et al., 2001).

Molecular Mechanism Mediating Tctex-1's Neurite Effect

Tctex-1 is known as a light chain of cytoplasmic dynein, a microtubule-based motor complex. Tctex-1's association with microtubules has been demonstrated both immunocytochemically and biochemically. Moreover, the ability of Tctex-1 in docking cargoes onto cytoplasmic dynein and, hence, microtubules has been confirmed (Tai et al., 1999; Tai et al., 2001).

However, several pieces of evidence described in this paper led us to propose that Tctex-1 is also involved in actin organization in undifferentiated neuroblasts and developing neurons. First, the Tctex-1 punctate signals at the filopodia edges of neurites were nicely colocalized with phalloidin-labeled microfilaments. The abundance of Tctex-1 at axonal tips correlates well with previous ultrastructural analysis showing a strong Tctex-1 signal in mossy fibers projecting to CA3 pyramidal neurons (Chuang et al., 2001). Second, Tctex-1 expression levels were inversely correlated with the abundance of F-actin: the level of overall F-actin labeling was significantly reduced in Tctex-1-overexpressing neurons. The loss of F-actin signal was especially profound at the neuronal tips, consistent with the notion that the actin filaments located in these regions of the neuron are generally more labile (Bradke and Dotti, 1999). In fact, the phalloidin staining of Tctex-1-transfected cells closely resembles that of cytochalasin D-treated hippocampal neurons. Third, the phenotype of multiple long axons induced by Tctex-1 overexpression can be, to a large extent, reversed by the coexpression with mutants of RhoGTPase proteins, prime regulators of actin reorganization. Finally, Tctex-1 levels modulate Rac1 activity. All together, these results indicate that Tctex-1 is not only physically associated, but also functionally involved, with both the microtubule and the microfilament cytoskeletal systems.

Our data also provide multiple lines of evidence arguing that dynein motor activity is not critical for Tctex-1-mediated neurite initiation and extension. First, the selective distribution of Tctex-1 in growing axons and the axonal tips was not shared by the DHC and DIC, implying that part of the "enriched" Tctex-1 signal may be free from the dynein complex. Second, p50 dynamitin overexpression and DHC gene silencing, which disrupts general dynein function, did not phenocopy the Tctex-1 knockdown effect. Third, Tctex-1 overexpression did not disrupt the integrity of the dynein complex, yet produced a dramatic phenotype. Fourth, the Tctex-1-mediated neuritic effect can be precisely reproduced by a phospho-mimic variant, T94E, which fails to incorporate into dynein. These results coherently suggested that the neuritic effect exerted by Tctex-1 is largely independent from its cargo adaptor role that is involved in dynein transport.

Nevertheless, the lack of a dramatic effect on neurite sprouting and axon formation in neurons with DHC expression/function suppressed does not necessarily indicate a lack of participation in these events, but may reflect the existence of some compensatory mechanism. Multiple dynein species or minus-end kinesins have been described, and some of them might be required for microtubule-based transport during neurite formation (Hirokawa, 2000) and axon retraction (Ahmad et al., 2000). In our experiments, impairing dynein activity by p50 overexpression in cultured hippocampal neurons causes swollen axons, consistent with the histological changes seen in the axons of motor neurons in p50-overexpressing transgenic mice (LaMonte et al., 2002). Finally, p50-overexpressing hippocampal neurons had slightly shorter axons (data not shown), consistent with those described in granule neurons overexpressing p50 (Solecki et al., 2004).

Molecular Basis Underlying Tctex-1 Regulation of Actin Dynamics

Our data suggest that Tctex-1 may participate in more than one step of actin/microtubule remodeling at the neurite growth cone. First, Tctex-1 could induce local actin instability, imitating the effect of cytochalasin D. Second, Tctex-1 could enhance F-actin and microtubule polymerization by locally activating Rac1. The latter possibility is highly conceivable because of the enrichment of Tctex-1 at the axonal growth cones and its ability to regulate Rac activity. Nevertheless, how Tctex-1 coordinates these steps of actin organization in still an open question.

A study of migrating fibroblasts suggests that microtubule growth activates Rac1 and hence actin polymerization (Waterman-Storer et al., 1999). The proteins preferentially associated with the plus-end of growing microtubules thus are good candidates to regulate Rac1 activity. Tctex-1 is also highly concentrated at microtubule plus ends (Tai et al., 2001). It is thus conceivable that Tctex-1 dissociates from the dynein complex near the microtubule growing end, perhaps via phosphorylation at Thr94, and locally activates Rac1. Our data show that the ectopically expressed unphosphorylated mimic T94A mutant is distributed in both the dynein complex and complex-free pools, but it has no axogenic effect. It is therefore likely that both the phosphorylation at Thr94 and its dissociation from the dynein complex are required for the "activation" of Tctex-1 for its neuritic role.

Tctex-1-enhancing Rac1 activity would be consistent with the fact that overexpressed Rac1 (this paper) or Tiam1 (Kunda et al., 2001) also enhanced neurite outgrowth and had an axogenic effect on hippocampal neuron cultures. Nevertheless, consistent with a previous report (Threadgill et al., 1997), Rac1 also induces lamellipodial wave structures located along axons and has a strong impact on primary dendrites that Tctex-1 does not have, indicating that Tctex-1 only participates in a subset of the Rac1 signaling pathways. These results also dovetail with our observations that Tctex-1 overexpression can only reverse the DN-Rac1-mediated axogenic, but not dendritic, effect. In addition, Tctex-1 suppression hardly inhibited the wave structures induced by CA-Rac1. The molecular link between the

regulator(s) of Rac1 and Tctex-1 is presently unknown. Tctex-1 itself is not likely to be a Rac1-GEF because it lacks a Dbl homology domain, which is required for GEF activity (Hart et al., 1991). Indeed, our unpublished observations showed that the Rac activation ability possessed by Tctex-1 was less potent than that possessed by Rac1GEFs, such as Tiam1. Tctex-1 most likely regulates Rac1 activity through an indirect pathway, such as recruiting RacGEF(s) and/or Rac effector(s). Alternatively, Tctex-1 may sequester RacGTPase activating protein (GAP) and enhance Rac1 activation. Many Tctex-1-interacting proteins have so far been isolated (reviewed in Vallee et al., 2004), and whether any of these proteins play roles in Tctex-1-mediated Rac activation remains an open question. Finally, because Rac and Rho activities feed back to each other, we cannot rule out the possibility that Tctex-1 may also attenuate Rho activity.

Although our knowledge about neurite extension has improved immensely in the past several years, relatively little is known about the mechanisms of the first step of neural development (reviewed in da Silva and Dotti, 2002; Dehmelt and Halpain, 2004). The inhibition of neurite initiation by Tctex-1 knockdown shown in this paper is dramatic; almost all neurons that had Tctex-1 suppressed were arrested at stage 1 in 24 hr cultures. More specifically, the Tctex-1-suppressed neurons resembled those at the substage called stage 1.2 (Dehmelt and Halpain, 2004). At stage 1.2, the lamellipodia are segmented and the microtubules have already invaded into the lamellipodia. These processes are in contrast to stage 1.1 cells, where lamellipodia are uniformly distributed around the circumference of the cell. The arrangement is also unlike stage 1.3 cells, which have microtubules aligned into parallel arrays (or bundles) at the selective segment. These results are in agreement with the hypothesis that microtubule polymerization takes place subsequent to actin disassembly, further supporting the role of Tctex-1 in regulating actin dynamics. Nevertheless, because the two cytoskeleton systems often feed back to each other (Wittmann and Waterman-Storer, 2001), future studies will be needed to examine the possibility that Tctex-1 could modulate microtubule stability and hence, microfilament dynamics.

Last but not least, it is our prediction that the dual function of Tctex-1 as a motor cargo adaptor in the microtubule transport system and a microfilament modulator is also very likely to be an important part of other cellular events (e.g., cell division, cell migration) that require a coordinated collaboration between the two cytoskeleton systems (Rodriguez et al., 2003).

Experimental Procedures

Antisense RNA, siRNA Oligonucleotide, Antibody, Plasmid Construct, and Virus Production

All antibodies, siRNAs, plasmids, and the details of their construction are listed in Supplemental Data. Adenoviruses encoding Tctex-1 and GFP were produced using the AdEasy system (Stratagene, La Jolla, CA). The shuttle vector was prepared by placing Tctex-1 into pTrack Shuttle vector (gift of Dr. B. Vogelstein, Johns Hopkins University). Adenovirus was amplified and purified as described (Tai et al., 2001). Adenovirus encoding GFP was a gift of Dr. F. Packe-Peterson (Weill Medical College, Cornell).

Culture, Transfection, and Immunochemical Analyses of Hippocampal Neurons

Embryonic hippocampal neuron cultures were prepared as described (Goslin and Banker, 1991). AS oligos (5 μM) were added twice into culture medium, at 2 hr and 12 hr after plating. For transfection, either plasmid (1–4 μg) or siRNA oligonucleotide (133 nM) were mixed with Lipofectamine 2000 and added into either freshly trypsin-dissociated hippocampal neurons, neurons 2 hr after plating, or neurons cultured 3 DIV. Neurons were

fixed at the indicated time and processed for immunolabeling as described (Paglini et al., 1998). FITC- or TRITC-phalloidin were added during the secondary antibody incubation. All immunostained cells were analyzed by Leica TCS SP2 spectral confocal system (Nussloch, Germany) or Zeiss confocal microscope. At least three independent experiments were conducted for each manipulation, with 15–40 coverslips and 50–100 cells examined in each experiment. Quantification of labeling intensities and morphometric analyses were carried out by using Metamorph software (Universal Imaging Co., Downingtown, PA) as described (Kunda et al., 2001). In some experiments, transfected neurons were cultured and prepared according to the procedures described by Paglini et al. (1998) for time-lapse imaging analysis.

Rac1 Activity Assays

Protein extracts of siRNA-transfected neurons or adenovirus-infected NIH 3T3 cells were subjected to Rac1 activity assays following the manufacturer's instructions (Cytoskeleton, Denver, CO). Briefly, the GTP bound form of Rac1 was affinity purified by GST agarose containing the Rac binding domain of Pak1. GTP bound Rac1 or total cell lysates were immunoblotted with anti-Rac1 anti-body (BD Transduction Lab, San Diego, CA) using ECL method.

Other Methods

Site-directed mutagenesis of Flag-Tctex-1 was carried out using Quickchange (Stratagene, La Jolla, CA). Velocity density gradient sedimentation, immunoprecipitation, and immunoblotting assays were carried out essentially as described (Tai et al., 1998).

Supplementary Material

Refer to Web version on PubMed Central for supplementary material.

Acknowledgments

We are indebted to the kind gifts given by our colleagues as mentioned in the text. This work was supported by Research To Prevent Blindness, The Irma T. Hirsch Trust, The Ruth and Milton Steinbach Fund, and NIH EY11307 to C.-H.S. and FONCyT, John Simon Guggenheim Foundation Fellowship, and the Howard Hughes Medical Institute (HHMI 75197-553201 International Research Scholars Program) to A.C.

References

Ahmad FJ, Hughey J, Wittmann T, Hyman A, Greaser M, Baas PW. Motor proteins regulate force interactions between microtubules and microfilaments in the axon. Nat. Cell Biol. 2000; 2:276–280. [PubMed: 10806478]

Baas PW, Ahmad FJ, Pienkowski TP, Brown A, Black MM. Sites of microtubule stabilization for the axon. J. Neurosci. 1993; 13:2177–2185. [PubMed: 8478694]

Bradke F, Dotti CG. The role of local actin instability in axon formation. Science. 1999; 283:1931–1934. [PubMed: 10082468]

Chuang JZ, Milner TA, Sung CH. Subunit heterogeneity of cytoplasmic dynein: differential expression of 14 kDa dynein light chains in rat hippocampus. J. Neurosci. 2001; 21:5501–5512. [PubMed: 11466421]

Corthesy-Theulaz I, Pauloin A, Pfeffer S. Cytoplasmic dynein participates in the centrosomal localization of the Golgi complex. J. Cell Biol. 1992; 118:1333–1345. [PubMed: 1387874]

da Silva JS, Dotti CG. Breaking the neuronal sphere: regulation of the actin cytoskeleton in neuritogenesis. Nat. Rev. Neurosci. 2002; 3:694–704. [PubMed: 12209118]

Dehmelt L, Halpain S. Actin and microtubules in neurite initiation: are MAPs the missing link? J. Neurobiol. 2004; 58:18–33. [PubMed: 14598367]

Dotti CG, Sullivan CA, Banker GA. The establishment of polarity by hippocampal neurons in culture. J. Neurosci. 1988; 8:1454–1468. [PubMed: 3282038]

Echeverri CJ, Paschal BM, Vaughan KT, Vallee RB. Molecular characterization of the 50-kD subunit of dynactin reveals function for the complex in chromosome alignment and spindle organization during mitosis. J. Cell Biol. 1996; 132:617–633. [PubMed: 8647893]

Esch T, Lemmon V, Banker G. Local presentation of substrate molecules directs axon specification by cultured hippocampal neurons. J. Neurosci. 1999; 19:6417–6426. [PubMed: 10414970]

Ferreira A, Busciglio J, Caceres A. Microtubule formation and neurite growth in cerebellar macroneurons which develop in vitro: evidence for the involvement of the microtubule-associated proteins, MAP-1a, HMW-MAP2 and Tau. Brain Res. Dev. Brain Res. 1989; 49:215–228.

Fletcher TL, Cameron P, De Camilli P, Banker G. The distribution of synapsin I and synaptophysin in hippocampal neurons developing in culture. J. Neurosci. 1991; 11:1617–1626. [PubMed: 1904480]

Forscher P, Smith SJ. Actions of cytochalasins on the organization of actin filaments and microtubules in a neuronal growth cone. J. Cell Biol. 1988; 107:1505–1516. [PubMed: 3170637]

Fukata M, Watanabe T, Noritake J, Nakagawa M, Yamaga M, Kuroda S, Matsuura Y, Iwamatsu A, Perez F, Kaibuchi K. Rac1 and Cdc42 capture microtubules through IQGAP1 and CLIP-170. Cell. 2002a; 109:873–885. [PubMed: 12110184]

Fukata Y, Itoh TJ, Kimura T, Menager C, Nishimura T, Shiromizu T, Watanabe H, Inagaki N, Iwamatsu A, Hotani H, Kaibuchi K. CRMP-2 binds to tubulin heterodimers to promote microtubule assembly. Nat. Cell Biol. 2002b; 4:583–591. [PubMed: 12134159]

Fukata Y, Kimura T, Kaibuchi K. Axon specification in hippocampal neurons. Neurosci. Res. 2002c; 43:305–315. [PubMed: 12135774]

Goslin, K.; Banker, G. Rat Hippocampal Neurons in Low-Density Culture. MIT; Cambridge, MA: 1991.

Hart MJ, Eva A, Evans T, Aaronson SA, Cerione RA. Catalysis of guanine nucleotide exchange on the CDC42Hs protein by the dbl oncogene product. Nature. 1991; 354:311–314. [PubMed: 1956381]

Hirokawa N. Kinesin and dynein superfamily proteins and the mechanism of organelle transport. Science. 1998; 279:519–526. [PubMed: 9438838]

Hirokawa N. Stirring up development with the heterotrimeric kinesin KIF3. Traffic. 2000; 1:29–34. [PubMed: 11208056]

Inagaki N, Chihara K, Arimura N, Menager C, Kawano Y, Matsuo N, Nishimura T, Amano M, Kaibuchi K. CRMP-2 induces axons in cultured hippocampal neurons. Nat. Neurosci. 2001; 4:781–782. [PubMed: 11477421]

Kai N, Mishina M, Yagi T. Molecular cloning of Fyn-associated molecules in the mouse central nervous system. J. Neurosci. Res. 1997; 48:407–424. [PubMed: 9185665]

King SJ, Schroer TA. Dynactin increases the processivity of the cytoplasmic dynein motor. Nat. Cell Biol. 2000; 2:20–24. [PubMed: 10620802]

Kunda P, Paglini G, Quiroga S, Kosik K, Caceres A. Evidence for the involvement of Tiam1 in axon formation. J. Neurosci. 2001; 21:2361–2372. [PubMed: 11264310]

LaMonte BH, Wallace KE, Holloway BA, Shelly SS, Ascano J, Tokito M, Van Winkle T, Howland DS, Holzbaur EL. Disruption of dynein/dynactin inhibits axonal transport in motor neurons causing late-onset progressive degeneration. Neuron. 2002; 34:715–727. [PubMed: 12062019]

Li MG, Serr M, Newman EA, Hays TS. The *Drosophila* tctex-1 light chain is dispensable for essential cytoplasmic dynein functions but is required during spermatid differentiation. Mol. Biol. Cell. 2004; 15:3005–3014. [PubMed: 15090621]

Luo L. Rho GTPases in neuronal morphogenesis. Nat. Rev. Neurosci. 2000; 1:173–180. [PubMed: 11257905]

Mok YK, Lo KW, Zhang M. Structure of Tctex-1 and its interaction with cytoplasmic dynein intermediate chain. J. Biol. Chem. 2001; 276:14067–14074. [PubMed: 11148215]

Nikolic M. The role of Rho GTPases and associated kinases in regulating neurite outgrowth. Int. J. Biochem. Cell Biol. 2002; 34:731–745. [PubMed: 11950591]

Paglini G, Kunda P, Quiroga S, Kosik K, Caceres A. Suppression of radixin and moesin alters growth cone morphology, motility, and process formation in primary cultured neurons. J. Cell Biol. 1998; 143:443–455. [PubMed: 9786954]

Ridley AJ, Paterson HF, Johnston CL, Diekmann D, Hall A. The small GTP-binding protein rac regulates growth factor-induced membrane ruffling. Cell. 1992; 70:401–410. [PubMed: 1643658]

Rodriguez OC, Schaefer AW, Mandato CA, Forscher P, Bement WM, Waterman-Storer CM. Conserved microtubule-actin interactions in cell movement and morphogenesis. Nat. Cell Biol. 2003; 5:599–609. [PubMed: 12833063]

Schwamborn JC, Puschel AW. The sequential activity of the GTPases Rap1B and Cdc42 determines neuronal polarity. Nat. Neurosci. 2004; 7:923–929. [PubMed: 15286792]

Shi SH, Jan LY, Jan YN. Hippocampal neuronal polarity specified by spatially localized mPar3/mPar6 and PI 3-kinase activity. Cell. 2003; 112:63–75. [PubMed: 12526794]

Shu T, Ayala R, Nguyen MD, Xie Z, Gleeson JG, Tsai LH. Ndel1 operates in a common pathway with LIS1 and cytoplasmic dynein to regulate cortical neuronal positioning. Neuron. 2004; 44:263–277. [PubMed: 15473966]

Solecki DJ, Model L, Gaetz J, Kapoor TM, Hatten ME. Par6alpha signaling controls glial-guided neuronal migration. Nat. Neurosci. 2004; 7:1195–1203. [PubMed: 15475953]

Tai AW, Chuang J-Z, Sung C-H. Localization of Tctex-1, a cytoplasmic dynein light chain, to the Golgi apparatus and evidence for dynein complex heterogeneity. J. Biol. Chem. 1998; 273:19639–19649. [PubMed: 9677391]

Tai AW, Chuang J-Z, Bode C, Wolfrum U, Sung C-H. Rhodopsin's carboxy-terminal cytoplasmic tail acts as a membrane receptor for cytoplasmic dynein by binding to the dynein light chain Tctex-1. Cell. 1999; 97:877–887. [PubMed: 10399916]

Tai AW, Chuang J-Z, Sung C-H. Cytoplasmic dynein regulation by subunit heterogeneity and its role in apical transport. J. Cell Biol. 2001; 153:1499–1509. [PubMed: 11425878]

Threadgill R, Bobb K, Ghosh A. Regulation of dendritic growth and remodeling by Rho, Rac, and Cdc42. Neuron. 1997; 19:625–634. [PubMed: 9331353]

Vallee RB, Williams JC, Varma D, Barnhart LE. Dynein: an ancient motor protein involved in multiple modes of transport. J. Neurobiol. 2004; 58:189–200. [PubMed: 14704951]

Waterman-Storer CM, Karki S, Holzbaur EL. The p150Glued component of the dynactin complex binds to both microtubules and the actin-related protein centractin (Arp-1). Proc. Natl. Acad. Sci. USA. 1995; 92:1634–1638. [PubMed: 7878030]

Waterman-Storer CM, Worthylake RA, Liu BP, Burridge K, Salmon ED. Microtubule growth activates Rac1 to promote lamellipodial protrusion in fibroblasts. Nat. Cell Biol. 1999; 1:45–50. [PubMed: 10559863]

Wittmann T, Waterman-Storer CM. Cell motility: can Rho GTPases and microtubules point the way? J. Cell Sci. 2001; 114:3795–3803. [PubMed: 11719546]

Zhou FQ, Zhou J, Dedhar S, Wu YH, Snider WD. NGF-induced axon growth is mediated by localized inactivation of GSK-3beta and functions of the microtubule plus end binding protein APC. Neuron. 2004; 42:897–912. [PubMed: 15207235]

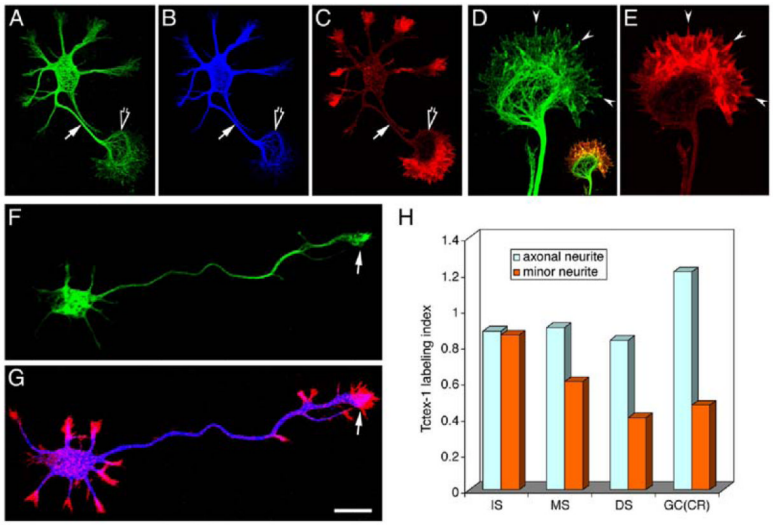

Figure 1.

Asymmetric Distribution of Tctex-1 in Hippocampal Neurons

(A–C) A stage 2–3 neuron immunostained for Tctex-1 (A), tyr-tubulin (B), and F-actin (C). Arrows point to the neurite of the future axon, and open arrows point to the axonal growth cones.

(D and E) Magnified views of axonal growth cones shown in (A) and (C). Arrowheads indicate the codistributed Tctex-1 and F-actin at the growth cone lamellipodia. Overlay is shown in the insert.

(F and G) Confocal images of a stage 3 neuron colabeled for Tctex-1 (F), tyr-tubulin (blue in [G]), and F-actin (red in [G]). Arrow marks the axon growth cone.

(H) Quantification of Tctex-1 expression levels in the neurites and growth cones of stage 2–3 neurons. The Tctex-1 labeling index represents the ratio of Tctex-1 labeling intensity relative to the tyr-tubulin labeling intensity. Both the minor neurites and the axonal neurites of these cells were subdivided into three even parts, which were designated as immediate segment (IS), middle segment (MS), and distal segment (DS), according to their distance from the cell body. The Tctex-1 labeling in the central regions (CR) of growth cones (GC) was also considered for quantification. However, the Tctex-1 labeling index in the peripheral regions of growth cones was not shown, because the tyr-tubulin labeling in these regions was often undetectable. n >100. Scale bars equal 10 μm in (A)–(C), (F), and (G) and 5 μm in (D) and (E).

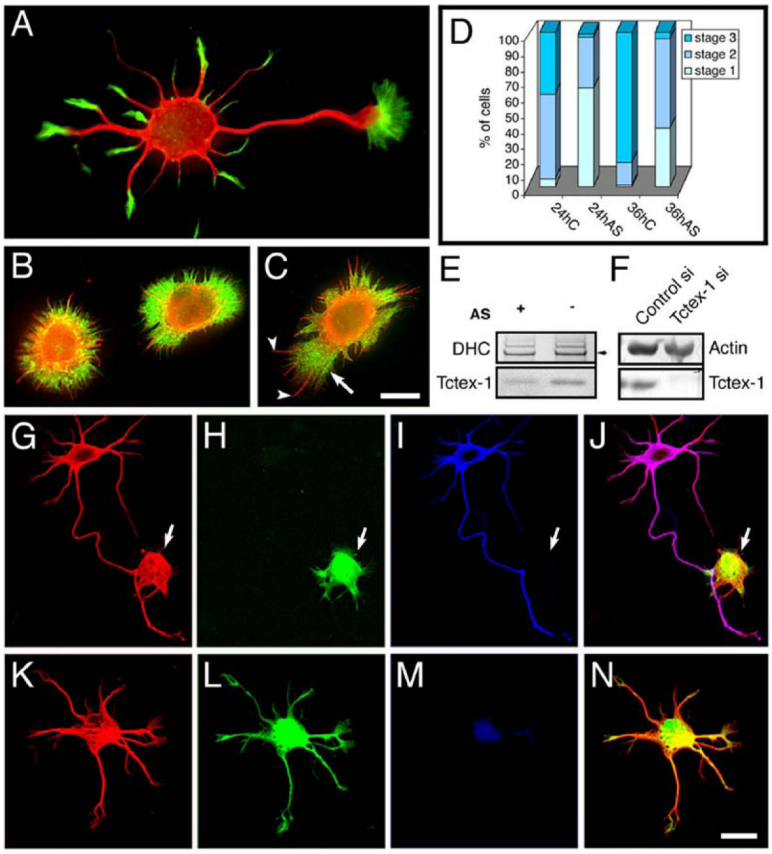

Figure 2.

Tctex-1 Suppression Inhibits Neurite Outgrowth

(A–C) Confocal images of neurons treated with a control AS for 24 hr (A), Tctex-1-AS for 24 hr (B), or Tctex-1-AS for 36 hr (C), followed by immunostaining for tyr-tubulin (red) and F-actin (green). The cell in (A) has the morphological appearance of stage 2–3 cell. In (C), arrow points to a segmented lamellipodium, and the arrowheads point to the short tubulin^{+} processes that penetrate the lamellipodial veil.

(D) Chart showing the percentage of cells at stage 1, 2, and 3 of neuritic development after a 24 hr or 36 hr treatment with control (C) or Tctex-1 AS-oligonucleotides. The scoring of stage 2 and stage 3 cells in control experiments were based on their typical morphological features (Dotti et al., 1988; Goslin and Banker, 1991). However, for the purpose of quantification, AS-treated cells carrying multiple tubulin^{+} processes with lengths similar to either minor neurites or axonal neurites were considered for classification, in spite of the fact that most of these processes are not typical neurites and lack growth cones.

(E and F) Immunoblotting of equal amount of proteins extracted from neurons treated with (+) or without (−) AS for 24 hr (E) or neurons transfected with control-siRNA/GFP or Tctex-1-siRNA/GFP (F) for 36 hr. The indicated antibodies were used.

(G–J) Neurons transfected with Tctex-1-siRNA/GFP 2 hr after plating and followed by immunostaining for TuJ1 (red) and Tctex-1 (blue) 22 hr later. GFP was visualized directly.

(K–N) An example of a typical neuron transfected with Tctex-1-siRNA/GFP ~15 hr after plating and immunolabeled 20 hr later. The cell has a weak Tctex-1 signal (blue) and a normal level of TuJ1 (red); it was arrested at stage 2 of neuritic development. Scale bar equals 10 μm.

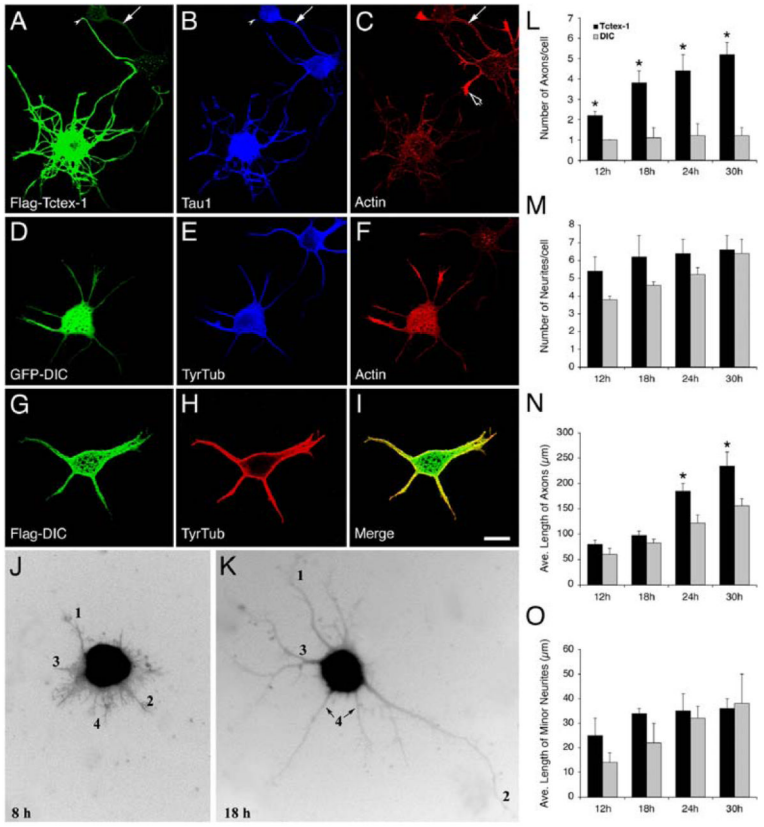

Figure 3.

Tctex-1 Overexpression Caused Multiple Long Axons in Hippocampal Cultures

(A–C) Dissociated neurons were transfected with Flag-Tctex-1 right before plating. Cells fixed 24 hr posttransfection were immunolabeled for Flag, Tau1, and phalloidin. The Flag-Tctex-1-transfected neurons exhibited abnormally long neurites and more than one are $Tau1^+$, whereas the nontransfected cells had one single $Tau1^+$ axon (arrow). Arrowheads indicated that $Tau1^+$ long neurites traveled long distances in and out of the focal plane. Note that cells ectopically expressing Tctex-1 consistently had much weaker labeling for phalloidin, particularly in the neurite tips. Open arrow points to the abundant phalloidin labeling at the neurite tips of untransfected neurons.

(D–I) Neurons transfected with GFP-DIC (D–F) or Flag-DIC (G–I) were immunolabeled as indicated 18 hr after transfection. Scale bar equals 10 μm.

(J and K) Time-lapse images of a live neuron cotransfected with GFP and Flag-Tctex-1 and imaged at 8 and 18 hr after plating. The numbers indicate neurites that elongated during the period of imaging.

(L–O) Histograms displaying the morphological analyses of cultures cotransfected with GFP/Flag-Tctex-1 or GFP/Flag-DIC (2 μg each) 2 hr after plating and processed for immunolabeling at the indicated time points posttransfection. A neurite that is $Tau1^+$ and ≥50 μm is considered to be an axon. Each value represents the mean ± SEM of at least 50 axonal processes for each experimental condition (*$p < 0.05$).

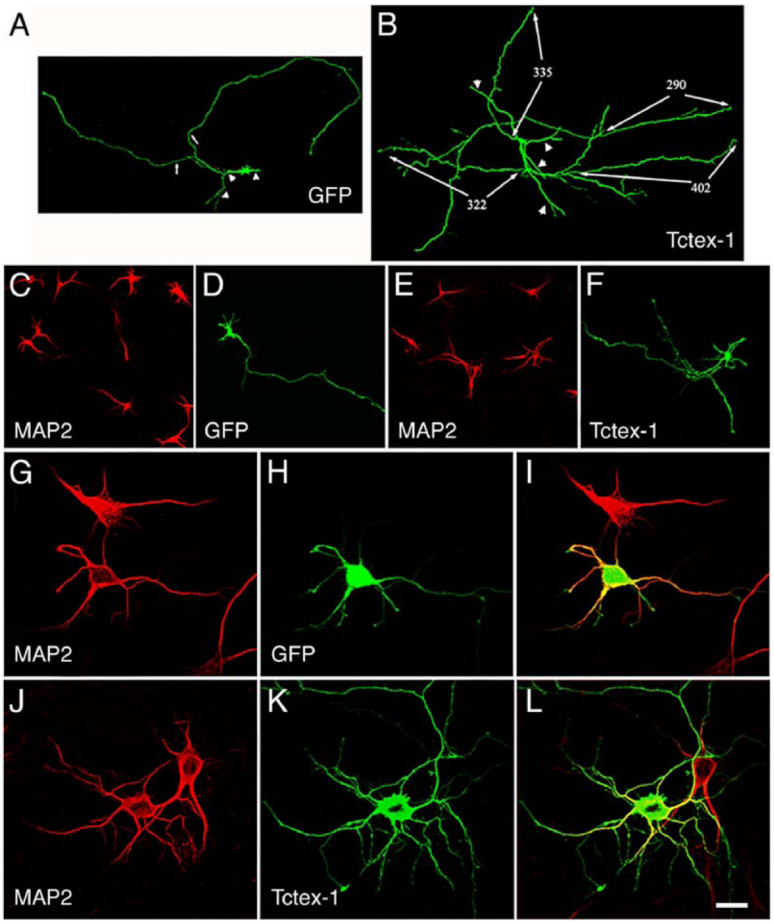

Figure 4.

Tctex-1 Regulates Both Axon and Dendrite Morphology in Older Neuronal Cultures

Cultures at 3 DIV were transfected with either GFP (2 μg) (A, C, D, G–I) or Flag-Tctex-1 (2 μg) (B, E, F, J–L) for 18 hr before processing. Neurons were either directly visualized for GFP (A, D, H), or immunolabeled for Flag (B, F, K) or MAP2 (C, E, G, J). Arrows and arrowheads in (A) and (B) point to axons and dendrites, respectively, based on their morphological features. The numbers in (B) correspond to the length of axonal processes. Scale bars equal 40 μm in (A)–(F) and 10 μm in (G)–(L).

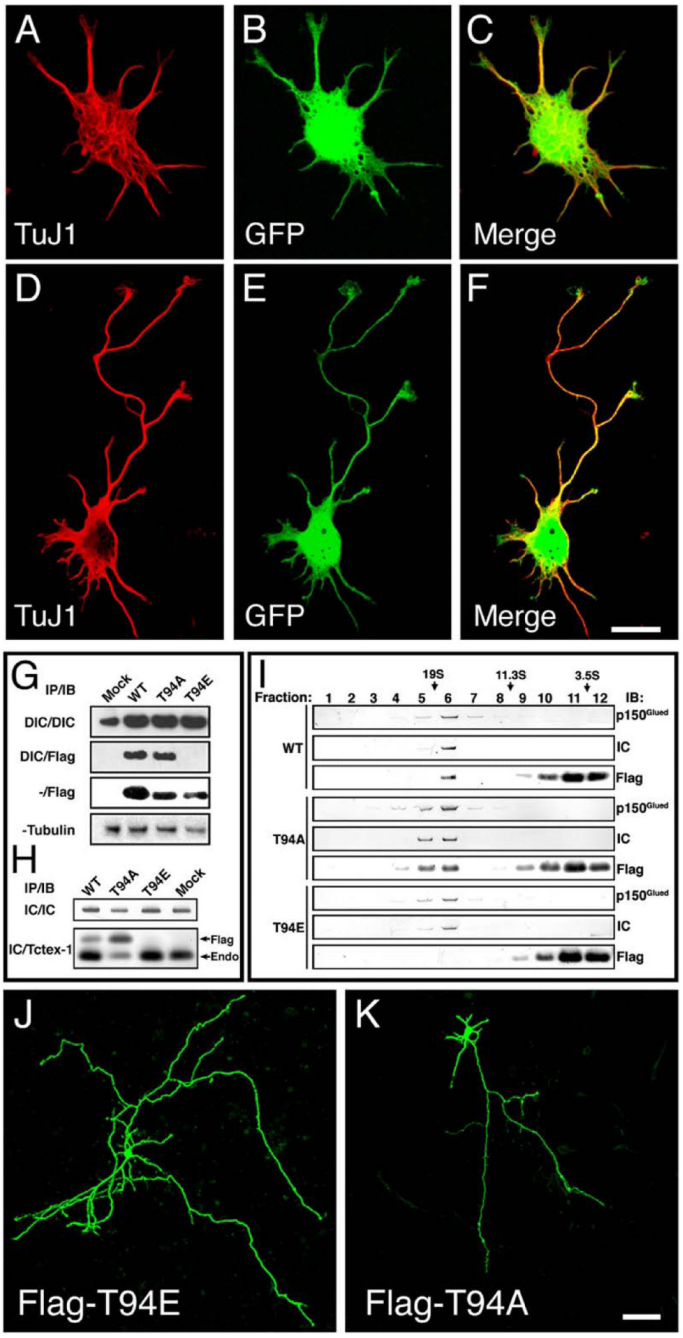

Figure 5.

Tctex-1's Neuritic Effect Is Dynein Independent

(A–F) Confocal images of 1 DIV neurons co-transfected with DHC-siRNA and GFP 2 hr after plating. The GFP+ targeted, TuJ1+ neurons were capable of reaching stage 2 (A–C) or 3 (D–F) of neuritic development.

(G) Immunoblots of the DIC immunoprecipitates obtained from mock-transfected 293T cells or 293T transfected with either Flag-WT, T94A, or T94E for either DIC or Flag. Total inputs are also shown.

(H) The DIC immunoprecipitates obtained from the 20 S fractions of (I) were immunoblotted with anti-DIC and anti-Tctex-1 Abs. Tctex-1 Ab recognized both Flag-tagged and endogenous (Endo) Tctex-1, which migrated differently.
(I) Lysates of 293T cells transfected with the either Flag-WT, T94A, or T94E were sedimented in a 5%–20% linear sucrose gradient. Each fraction was analyzed by SDS-PAGE and immunoblotted with indicated Abs.
(J and K) Immunolabeling of 4 DIV neurons transfected with Flag-T94E and Flag-T94A using anti-Flag Ab. Scale bars equal 10 μm.

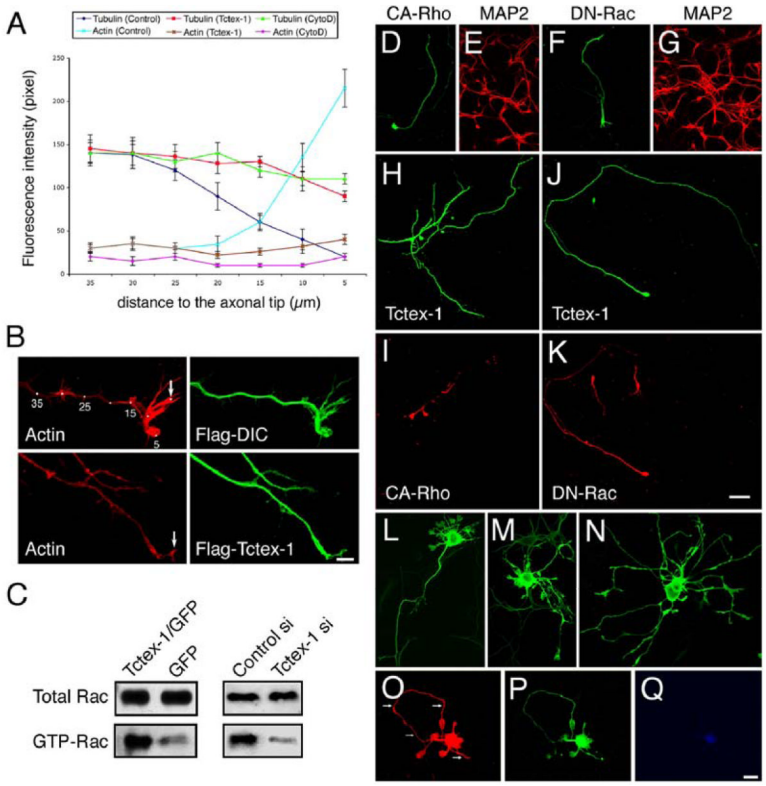

Figure 6.

Tctex-1 Regulates the Actin Cytoskeleton by Modulating RhoGTPase

(A) Quantification of F-actin and tubulin fluorescence intensity at the neuritic tip of 1 DIV control neurons, neurons transfected with Flag-Tctex-1, or neurons treated with cytochalasin D (0.5 μg/ml) for 6 hr. Measurements were performed pixel by pixel (y axis) along the distal end of axonal processes (x axis). Values of representative measurements taken at 5 μm intervals are shown in the graph. Each value represents the mean ± SEM of at least 50 axonal processes for each experimental condition.

(B) Representative images of distal axonal processes of neurons transfected with Flag-DIC and Flag-Tctex-1 and labeled for F-actin and Flag. All images were taken using identical confocal settings to quantify paladin labeling. Arrows mark the axonal tips for the zero points used in the quantification described in (A).

(C) Equal amounts of protein extracted from 3T3 fibroblasts infected with adenovirus encoding Tctex-1/GFP or GFP (left) or neurons transfected with Tctex-1-si/GFP or control-si/GFP (right) were subjected to the Rac1 activity assay. A representative immunoblot shows the total and GTP bound Rac1.

(D–K) 1 DIV neurons singly transfected with either HA-CA-RhoA (D, E) or HA-DN-Rac1 (F, G) or double-transfected with Tctex-1/HA-CA-RhoA (H, I) or Tctex-1/HA-DN-Rac1. (J) and (K) were immunolabeled for either HA (D, F, I, K) together with MAP2 (E, G) or together with Flag (H, J).

(L–N) Confocal images of cultured neurons transfected with 1 μg (L), 2 μg (M), or 4 μg (N) of myc-CA-Rac1 and labeled with anti-myc Ab.

(O–Q) Confocal images showing the morphology of a neuron cotransfected with myc-CA-Rac1 and Tctex-1-si/GFP (2 μg each; red, myc; green, GFP; blue, Tctex-1). Note that the transfected neuron, which displays very faint Tctex-1 immunofluorescence, extended a single axon (arrows) and several “veiled” shorter neurites. All cells shown in this figure were transfected 2 hr after plating and fixed 24 hr later. Scale bars equal 10 μm.

Table 1

Quantative Analyses of Morphological Changes of Transfected Neurons

Overexpressed Protein	Number Axons	Mean Axonal Length	Number Dendritic Branches	Mean Dendritic Length
GFP	1.24 ± 0.2	720 ± 38	8.4 ± 1.8	238 ± 24
Tctex-1-WT (2 μg)	2.45 ± 0.3*	2113 ± 219*	18.6 ± 2.2*	604 ± 18*
Tctex-1-WT (1 μg)	1.85 ± 0.2*	1228 ± 46*	14.2 ± 2.4*	378 ± 28*
T94E	2.21 ± 0.2*	1915 ± 147*	16.8 ± 1.6*	524 ± 34*
T94A	1.38 ± 0.2	840 ± 26	9.2 ± 1.2	256 ± 16
CA-Rho	1.08 ± 0.2	240 ± 16*	4.2 ± 0.8*	80 ± 12*
DN-Rac	1.20 ± 0.2	298 ± 24*	2.4 ± 0.8*	40 ± 10*
Tctex-1 + CA-Rho	1.20 ± 0.2	585 ± 84	6.2 ± 0.6	220 ± 46
Tctex-1 + DN-Rac	1.1 ± 0.2	510 ± 68	2.2 ± 0.2*	68 ± 10*

All measurements were performed at 4 DIV. Cells were transfected at 3 DIV (at which time point the mean axonal length of control cells was 540 ± 62 μm) and fixed 18–20 hr later. 2 μg of plasmid was typically used, except 1 μg of Tctex-1 was used in one set of experiments to demonstrate the dosage effect. Each value represents the mean ± SEM of at least 50 cells for each experimental condition. Asterisk represents value significantly different from that of GFP-transfected control neuron ($p < 0.01$) as determined by one-way ANOVA.